

1 development [1]. Commercial users have full access to professional services of the ANKA facility and the FZK
2 infrastructure on a contractual basis via ANKA's Commercial Service department (ANKA COS) [2].

3 In 2005 an X-ray imaging group has been established within the ISS for the development of instrumentation and
4 methods and their application in scientific users' and commercial customers' projects. Currently a bending
5 magnet beamline named TopoTomo is available for imaging, a dedicated insertion device beamline is under
6 construction and further experimental stations are accessible via external cooperations (University of Karlsruhe,
7 European Synchrotron Radiation Facility). A cooperation with the Fraunhofer Institut für Techno- und
8 Wirtschaftsmathematik (Kaiserslautern, Germany) is the basis for development and application of quantitative
9 image analysis methods on three-dimensional (3D) volume data [3]. The imaging group also has a leading role in
10 a European research project for the development of novel X-ray detectors based on thin scintillating crystals
11 (SCIN^{TAX} - <http://www.scintax.eu>). These detectors will be characterized and used at TopoTomo for topography,
12 micro-tomography and –radiography [21, 22].

13 **2. White beam synchrotron X-ray topography and diffraction imaging**

14 White beam synchrotron X-ray topography is a non-destructive characterisation method for defects and strain in
15 bulk crystals, electronic devices and epitaxial layers. The strength of the method is the easy operation in
16 combination with high spatial resolution. The principle idea is sketched in figure 1: the white beam is diffracted
17 by a crystal. Every diffraction vector which fulfils Bragg's law results in one topograph from the same sample
18 area, by using X-ray films one can record a Laue pattern of topographs with one single exposure. Every
19 inhomogeneity (e.g. dislocations) in the crystal structure leads to a violation of Bragg's law and therefore to an
20 intensity modification in the corresponding topograph. An example of a topograph can be seen in figure 2 (left)
21 [4, 5]. Large area and section topography allow for a quantitative analysis of the type of dislocations and the
22 dislocation density. For highly absorbing materials the back reflection geometry is applied to investigate
23 dislocation networks and small angle grain boundaries. A grazing incidence method is used to characterise strain
24 and defects as a function of depth by varying the tilt of the sample [4, 5].

25 X-ray films are frequently used to record a Laue pattern of topographs due to their large field of view, high
26 sensitivity and high resolution. The rather long post-processing time of X-ray films usually do not allow for an
27 automatisisation and also high resolution films tend to disappear more and more from the market. High resolution

1 imaging pixel detectors are one approach to replace X-ray films. They combine comparable spatial resolution,
2 high dynamic range and high frame repetition rates [7, 8]. As their field of view is limited (see as example figure
3 2 – left), moving the detector to different positions is required to obtain a complete Laue pattern of topographs
4 [8]. An application of this so-called digital white beam synchrotron X-ray topography is to record a selected
5 topograph, e.g. of a large wafer, and via a mapping to image stress, strains or dislocations over the whole wafer
6 area (for up to 300 mm diameter) – see figure 2 (right) [6].

7 X-ray topography can be extended to more general full field micro-diffraction imaging schemes, e.g. rocking
8 curve imaging. Here, rocking curves corresponding to different areas of the sample are measured by recording
9 classical topographs with a monochromatic synchrotron beam while tilting the sample around a rocking angle –
10 see figure 3 (top). By analysing the rocking curves one can measure stress, mosaicity and curvature in any kind
11 of crystalline structure, e.g. again to be applied to wafers in order to optimize the fabrication technology. This
12 technique is very promising for quality imaging of microelectronic devices [9].

13 **3. Synchrotron micro-radiography and -tomography**

14 Micro-radiography and -tomography are well-established methods for the non-destructive evaluation and
15 materials research [10, 11]. The use of synchrotron radiation instead of laboratory sources for tomography and
16 radiography allows to extend the resolution to the sub-micrometre scale, to reduce noise, beam hardening and
17 cone beam artefacts as well as increasing the contrast by the use of monochromatic radiation [7, 10, 11, 12, 13] –
18 see also figure 4. This is due to the nearly parallel beam propagation and intense flux of synchrotron light
19 sources. Additionally, synchrotron light has a degree of spatial coherence that allows to use interference effects,
20 e.g. phase contrast and holo-tomography, in order to increase the contrast [11, 14]. High resolution and phase
21 contrast radiography are used to investigate micro-structured, multi-component material systems, e.g. to detect
22 delaminations between substrates and glob tops encapsulating wire-bonded devices. Radiographs taken from
23 different projection angles for computed micro-tomography allow to image objects in three dimensions with a
24 spatial resolution up to the sub-micrometre range, e.g. bio-ceramics in regenerating bone tissue. Subsequent 3D
25 image analysis, for example by methods derived from stochastic geometry, can be used for the determination of
26 size distributions, orientations or spatial correlations within tomographic, multi-constituent volume images [3].

27 At ANKA we use two different optical systems for the indirect detection of X-rays by projecting the

1 luminescence image of a scintillator magnified via visible light microscope optics onto, for example, a CCD.
2 One is optimised for moderate resolutions and large fields of view used to image bigger objects with more than 1
3 cm diameter (macroscope). The second one is optimised for highest resolutions down to sub-micrometre scale.
4 These optics can be combined with different digital cameras depending on the application. A commercially
5 available PCO.4000 (PCO AG / Cooke Cooperation) with a large (11 megapixel, interline transfer CCD) chip
6 can be used with the macroscope as well as for high resolution with the microscope in order to extend the field of
7 view. A FReLoN *2k14bit* fulfils the needs for high dynamic tomographic scans with short exposure times
8 ($\ll 1$ s) and a high duty cycle, e.g. with the microscope system and 8x to 20x magnification [23].

9 Currently high speed CMOS cameras are applied by the ISS imaging group with the aim to being able to work
10 with frame rates of several thousand images per second employing a one megapixel chip and spatial micro-
11 resolution. By using a region of interest, frame rates of several 10 000 FPS are possible [20]. Additionally
12 ANKA and the ESRF developing together the FReLoN *2k14bit* further in order to increase the cameras
13 efficiency down to 400 nm, allowing one to achieve higher resolutions and to use faster and more denser
14 scintillating materials. A first new FReLoN will be commissioned in the second half of 2008.

15 **4. Synchrotron computed laminography**

16 Micro-tomography is limited to scan objects which fit into the field of view of the imaging system. Objects
17 which are slightly bigger than the field of view can be used as well (local tomography), frequently introducing
18 artefacts. In order to obtain volume image data of laterally extended samples, digital laminography for laboratory
19 applications was implemented in the 1990s. Here, an X-ray source is rotated around the flat sample with an
20 inclined angle of projection [15]. Recently, synchrotron computed laminography has been developed and
21 implemented at the ESRF beamline ID19 by members of the ISS Imaging group in order to image flat and
22 laterally extended objects with high spatial resolution in three dimensions. Due to the fact that the synchrotron
23 radiation source is fixed, the sample is rotated with an inclined axis of rotation (cf. figure 4 (top, right) –
24 laminography and CT - left). The inclined axis of rotation results in a different scanning of the Fourier space (see
25 figure 4 – bottom), omitting some spatial frequencies but allowing one to image flat extended samples in three
26 dimensions. Flip-chip bonded and wire-bonded devices are examples which show the potential of this method
27 for typical industrial micro system application like the detection of mm-sized voids within solder bumps [16].

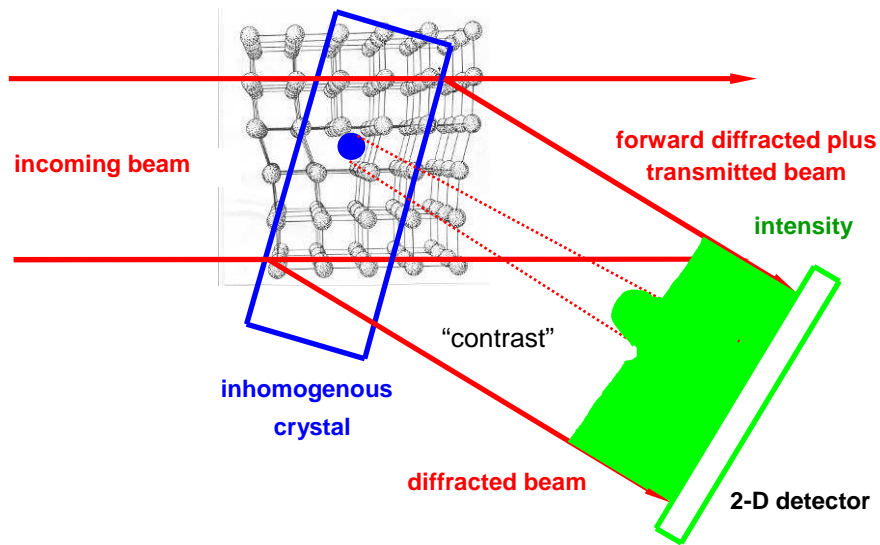
1 5. Summary

2 This article gives a short overview of imaging methods for industrial applications accessible via our department
3 ANKA Commercial Service (ANKA COS) [2]. Further imaging activities at ANKA which have not been
4 mentioned in detail in this article are the development and production of refractive lenses fabricated by deep
5 synchrotron radiation lithography [17], fluorescence imaging [18] and the construction of an insertion device
6 beamline at ANKA, dedicated to host different imaging methods [1].

7 *This contribution was funded by the CAARI2008 local organizing committee.*

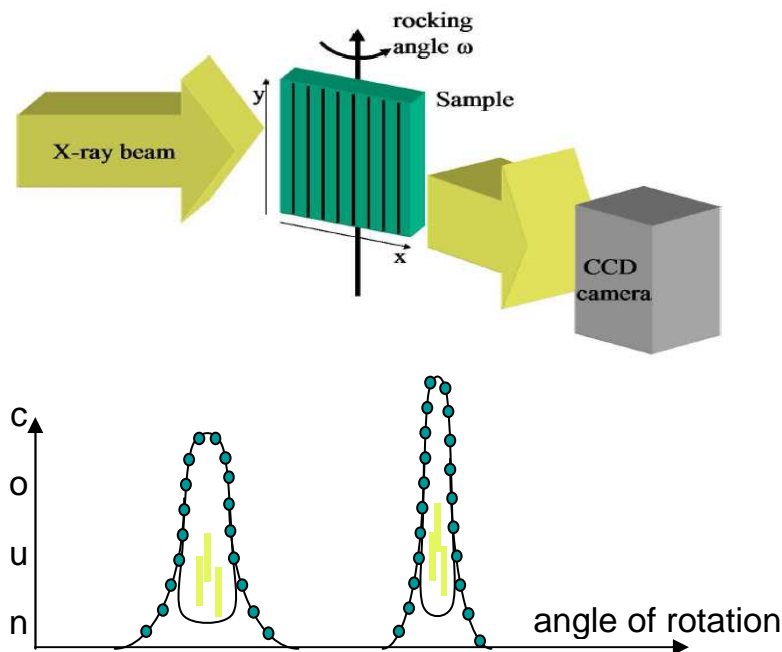
- 8 1. <http://www.fzk.de/anka/> – last visit July 2008, ANKA Instrumentation Book (November 2007/3).
- 9 2. <http://www.anka-cos.de/> – last visit July 2008.
- 10 3. <http://www.itwm.fhg.de/mab/projects/MAVI/> – last visit July 2008.
- 11 4. T. Tuomi, K. Naukkarinnen, P. Rabe, Phys. Stat. Sol. (a), 25 (1974), 93.
- 12 5. R. Simon, A. N. Danilewsky, Nucl. Instr. & Meth. Phys. Res. B 199 (2003), p. 550.
- 13 6. A. N. Danilewsky, J. Wittge, A. Rack, T. Weitkamp, R. Simon, P. McNally, J. Mat. Sci.: Mat. in Electr.
14 *in print* (2008), DOI 10.1007/s10854-007-9480-5.
- 15 7. U. Bonse, F. Busch, Prog. Biophys. Molec. Biol. 65 (1996), p. 133.
- 16 8. A. N. Danilewsky, A. Rack, J. Wittge, T. Weitkamp, R. Simon, H. Riesemeier, T. Baumbach, Nucl.
17 Instr. & Meth. Phys. Res. B 266 (2008), p. 2035.
- 18 9. D. Lübbert, T. Baumbach, J. Härtwig, E. Boller, P. Pernot, Nucl. Instr. & Meth. Phys. Res. B 160
19 (2000), p. 521.
- 20 10. J. Goebbels, B. Illerhaus, Y. Onel, H. Riesemeier, G. Weidemann, in: Proc. 16th World Conference on
21 Nondestructive Testing (WCNDT2004), Montreal, Canada, (2004),
22 www.ndt.net/article/wcndt2004/pdf/radiography/559_goebbels.pdf .

- 1 11. J. Banhart (Ed.), 'Advanced Tomographic Methods in Materials Research and Engineering', Oxford
2 University Press, Oxford, 2008.
- 3 12. B. P. Flannery, H. W. Deckmann, W. G. Roberge, K. L. D'Amico, *Science* 237 (1987), p. 1439.
- 4 13. A. Koch, C. Raven, P. Spanne, A. Snigirev, *J. Opt. Soc. Am.* 15 (1998), p. 1940.
- 5 14. P. Cloetens, W. Ludwig, J. Baruchel, D. Van Dyck, J. Van Landuyt, J. P. Guigay, M. Schlenker, *Appl.*
6 *Phys. Lett.* 75 (1999), p. 2912.
- 7 15. U. Ewert, J. Robbel, C. Bellon, A. Schumm, C. Nockemann, *Materialforschung* 37 (1995), p. 218.
- 8 16. L. Helfen, T. Baumbach, T. Mikulik, D. Kiel, P. Pernot, P. Cloetens, J. Baruchel, *Appl. Phys. Lett.* 86
9 (2005), 071915.
- 10 17. V. Nazmov, E. Reznikova, M. Boerner, J. Mohr, V. Saile, A. Snigirev, I. Snigireva, M. DiMichiel, M.
11 Drakopoulos, R. Simon, M. Grigorie, *AIP Conference Proceedings (SRI2004)* 705 (2004), p. 752.
- 12 18. R. Simon, G. Buth, M. Hagelstein, *Nucl. Instr. & Meth. Phys. Res. B* 199 (2003), p. 554.
- 13 19. X-ray diffraction imaging (X-ray topography) –
14 <http://www.esrf.fr/UsersAndScience/Experiments/Imaging/ID19/Techniques/Diffraction/Overview> (last visit
15 August 2008).
- 16 20. F. Garcia Moreno, A. Rack, L. Helfen, T. Baumbach, S. Zabler, N. Babcsan, J. Banhart, T. Martin, C.
17 Ponchut, M. Di Michel, *Appl. Phys. Lett.* 92 (2008), 134104.
- 18 21. K. Dupré, M. Couchaud, T. Martin, A. Rack, German Patent Application, ref. no. 10 2007 054 700.7
19 (2007).
- 20 22. A. Cecilia, A. Rack, T. Baumbach, P.-A. Douissard, T. Martin, M. Couchaud, K. Dupré, J.
21 Luminescence, *submitted* (2008).
- 22 23. J.-C. Labiche, O. Mathon, S. Pascarelli, M. A. Newton, G. Guilera Ferre, C. Curfs, G. Vaughan, A.
23 Homs, D. F. Carreiras, *Rev. Sci. Instr.* 78 (2007), 091301.



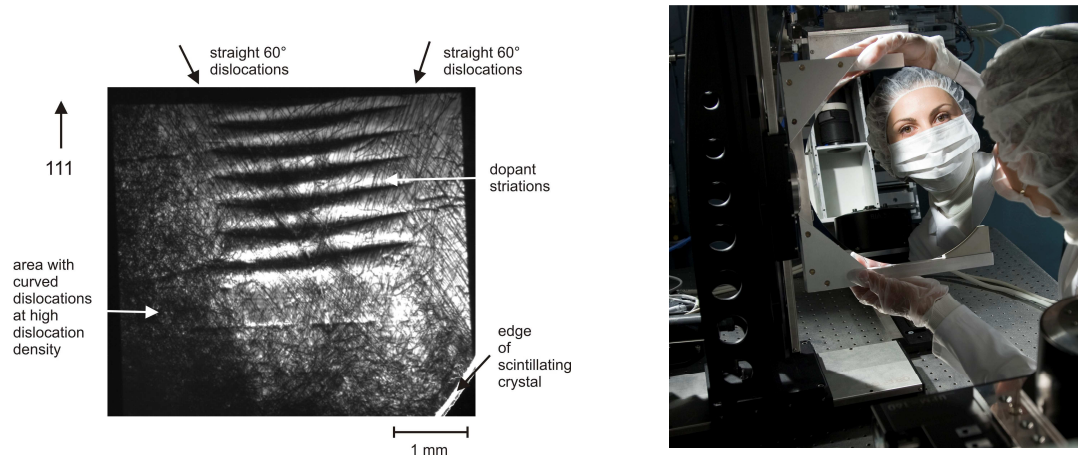
1
2 Figure 1. Contrast in X-ray topography: defects in a single-crystal do not fulfil the Bragg condition for a selected
3
4 diffracted beam, which leads to a change of intensity in the corresponding topograph (Figure courtesy

5
6 J. Härtwig, ESRF) [19].



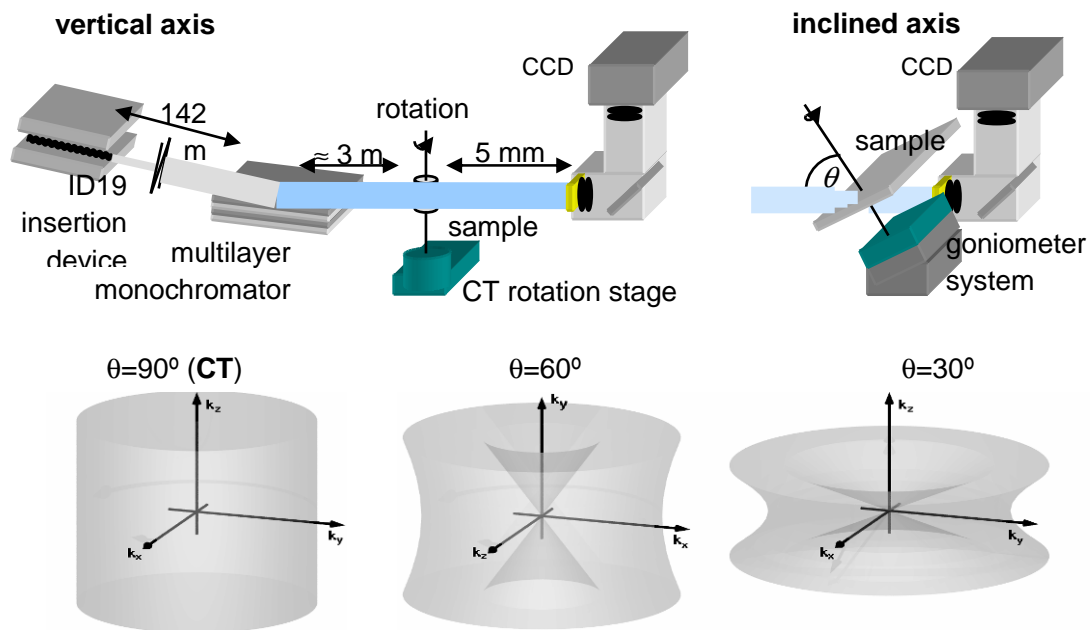
7
8 Figure 3. Top: rocking curve imaging - a monochromatized synchrotron radiation beam is diffracted by the
9 sample; the spatial variation of the diffracted intensity over the surface of the sample is recorded by a pixel
10 detector (classical topography). By recording a series of such images for different sample rocking angles, a
11 whole set of rocking curves can be measured simultaneously. Bottom: rocking curve analysis – Bragg position
12
13 (misorientation, stress), FWHM (dislocations, macrodefects, stress, inclusions) [9].
14
15
16

1



2 Figure 2. Left: digitally recorded 111 topograph of a highly sulphur doped InP crystals [8]. Right: experimental
 3 stage for mapping large wafers (up to 300 mm diameter) with digital white beam synchrotron X-ray topography
 4 [6].
 5
 6

7



8
 9 Figure 4. Top: Sketch of the synchrotron micro-tomography facility at the beamline ID19 of the ESRF [14] (left)
 10 and modified setup for synchrotron laminography [16] (right). Bottom: comparison of sampling Fourier space
 11
 12 for micro-tomography (CT) and laminography (inclined axis of rotation) [16].
 13